Sub-barrier fusion of neutron-rich nuclei and its astrophysical consequences

V. I. Zagrebaev and V. V. Samarin
Flerov Laboratory of Nuclear Reactions, JINR, Dubna, Moscow Region, Russia

Walter Greiner
Frankfurt Institute for Advanced Studies, J. W. Goethe-Universität, Frankfurt, Germany

(Received 15 December 2006; revised manuscript received 8 February 2007; published 27 March 2007)

Near-barrier fusion of neutron-rich nuclei was studied within the semiempirical channel coupling model for intermediate neutron rearrangement and within the time-dependent three-body Schrödinger equation. The possibility of neutron transfer with positive Q values considerably increases the barrier penetrability. A huge enhancement of deep sub-barrier fusion probability was found for light neutron-rich weakly bound nuclei (such as ^{6}He). This may be quite important for astrophysical primordial and supernova nucleosynthesis.

DOI: 10.1103/PhysRevC.75.035809 PACS number(s): 25.70.Jj, 25.60.Pj, 26.30.+k

I. INTRODUCTION

The reactions with neutron-rich nuclei have recently received increased interest as well experimentally as theoretically. The possibility to perform experiments with neutron-rich radioactive fission fragments [1] opens new doors for the production and study of new isotopes and, probably, for synthesis of new superheavy elements. Also great efforts have been devoted to studying near-barrier fusion of light weakly bound nuclei [2–7]. Unusual effects are expected here both from the halo structure of these nuclei and from the specific tunneling mechanism of the composed weekly bound system that is of general interest for quantum theory [8].

Neutron transfer cross sections are known to be rather large at near-barrier energies of heavy-ion collisions—the result of significant extension of the wave functions of neutrons from the outer nuclear shells (we call them "valence neutrons"). As a consequence there is a prevailing view that coupling with the transfer channels should play an important role in sub-barrier fusion of heavy nuclei. However, if an influence of collective excitations (rotation of deformed nuclei and surface vibrations) on near-barrier fusion of heavy nuclei is well studied experimentally and well understood theoretically, the role of neutron transfer is not so clear.

Such a situation can be explained by a series of difficulties. First, in the experimental study of the effect, one needs to compare the fusion cross sections of different combinations of nuclei, which among other things have different collective properties. Therefore it is not so easy to single out the role of neutron transfer from the whole effect of sub-barrier fusion enhancement. Second, it is very difficult, for many reasons, to take into account explicitly the transfer channels within a consistent channel coupling (CC) approach used successfully for the description of collective excitations in the near-barrier fusion processes. As a result, we are still far from a good understanding of the subject.

Some time ago Stelson *et al.* [9] proposed an empirical distribution of barriers technique and found that many experimental data may be well described by a flat distribution of barriers with a lower-energy cutoff, which corresponds to the energy at which the nuclei come sufficiently close together for neutrons to flow freely between the target and projectile (neck formation). There is no doubt that flow of neutron matter into or out of the region between the target and projectile regulates somehow the fusion process. However, from recent experiments it becomes clear that the neutron excess may increase the nuclear radius, thus decreasing the height of the Coulomb barrier. But the reduced fusion cross sections (plotted as a function of the ratio of center-of-mass energy to the Coulomb barrier) demonstrate more or less the same behavior at near-barrier region even for very neutron-rich systems like ^{64}Ni+^{132}Sn as compared with ^{64}Ni+$^{112-124}$Sn [10] and ^{38}S +^{208}Pb as compared with ^{32}S +^{208}Pb [11]. Moreover, for some combinations fusion of neutron rich isotopes was found to be less probable than fusion of the same nuclei with smaller number of neutrons. For example, sub-barrier fusion probability for ^{48}Ca+^{48}Ca is less than for ^{40}Ca+^{48}Ca [12]. The same holds for ^{48}Ca +^{96}Zr [13] as compared with ^{40}Ca +^{96}Zr. Thus we may definitely conclude that the neutron excess *itself* does not lead to additional fusion enhancement.

At the same time more and more experimental data appear testifying additional sub-barrier fusion enhancement due to neutron transfer with positive Q values. Indeed, in all the neutron-rich combinations listed above, ^{48}Ca+^{48}Ca, ^{48}Ca +^{96}Zr, ^{38}S +^{208}Pb, ^{64}Ni+^{132}Sn, intermediate neutron rearrangement may occur only with negative or very small Q values. However, if one compares the fusion cross sections of ^{18}O+^{58}Ni ($Q_{2n} = +8.5$ MeV) with ^{16}O+^{60}Ni [14], ^{40}Ca+^{48}Ca ($Q_{4n} = +3.9$ MeV) with ^{48}Ca +^{48}Ca [12], and ^{40}Ca +^{96}Zr ($Q_{2n} = +5.5$ MeV) with ^{40}Ca+^{90}Zr [15], one may find that in all the cases sub-barrier fusion turns out to be more probable just for those combination in which an intermediate neutron rearrangement with positive Q value is possible (see below).

The role of neutrons should be even more important in fusion of light neutron-rich weakly bound nuclei. Some model calculations predicted that the weak binding energy of the nuclei should significantly suppress the near-barrier fusion cross section [16–19]. However, the extended "halo" structure of exotic nuclei, such as ^{6}He or ^{11}Li, may also influence the fusion probability. In Refs. [20–23] some enhancement of the fusion probability for weakly bound nuclei was found due to the excitation of a low-lying soft-dipole mode and due to the

strong coupling with the breakup channels. See also the recent review articles on the problem of fusion of weakly bound nuclei [24,25].

An experimental situation is also quite uncertain. A significant enhancement was reported for the ^{6}He + ^{209}Bi fusion reaction compared to the one expected according to the standard model [2,3]. The same was also found at first for sub-barrier fusion of ^{6}He with ^{238}U as compared with fusion of ^{4}He [4]. However, it is rather difficult to make an unambiguous interpretation of these results. In the ^{4,6}He+^{209}Bi fusion reactions compound nuclei are produced that differ both in excitation energies and decay properties, which makes it difficult to compare directly the yields of evaporation residues. In a fusion-fission reaction such as ^{6}He +^{238} U (with detection of fission fragments only) it is difficult to distinguish the process of complete fusion from other channels contributing to the total yield of the fission fragments. Finally it was concluded that the observed enhanced yield of the fission fragments in this reaction at sub-barrier energies could be attributed mainly to $2n$-transfer reactions to the excited states of ^{240}U (with its subsequent fission) and, thus, there is no enhancement at all of the fusion probability for ^{6}He [6]. Thus, no matter how surprising it may seem, but until now there is no consensus (neither in theory nor in experiment) on the extent to which the sub-barrier fusion of weakly bound nuclei differs from fusion of ordinary ones.

In this article we study an influence of intermediate neutron rearrangement on the sub-barrier fusion of atomic nuclei. In Sec. II we use the semiempirical channel coupling approach to analyze available experimental data on fusion of neutron-rich nuclei and make some predictions. In Sec. III we solve numerically a time-dependent three-body Schrödinger equation to find more clear answers on the two questions. (1) What happens with valence neutrons when nuclei approach each other? (2) How influences the rearrangement of valence neutrons on fusion of nuclei? Astrophysical consequences of a possible deep sub-barrier fusion enhancement for light neutron rich nuclei is discussed in Sec. IV.

II. NEUTRON REARRANGEMENT WITH POSITIVE Q VALUE

As mentioned above, for some combinations of nuclei neutron transfers with positive Q value are possible. It is rather difficult (if possible at all) to use the standard CC method for the description of the process of neutron transfer in fusion reactions (partly due to impossibility of a choice of a complete set of the orthogonal basic functions for a decomposition of the total wave function). That is why the semiempirical channel coupling [26,27] and semiclassical [28] models have been recently proposed to study an influence of neutron transfers on a fusion process. In Ref. [28] it was assumed that the particle transfer degrees of freedom lead only to additional spread of the dissipated energy and play a minor role, whereas the sub-barrier fusion enhancement is mainly due to the adiabatic polarization term caused by the surface vibrations. In contrast with this, in the models proposed in Refs. [26] and [27] it is a gain in energy obtained due to an intermediate neutron transfer with $Q > 0$, which may additionally increase the sub-barrier fusion probability.

The fusion cross section may be estimated rather accurately using the concept of so-called "barrier distribution function," $f(B)$, arising due to the multidimensional character of the real nucleus-nucleus interaction. The quantum penetrability of the Coulomb barrier is calculated here in the following way: $T(E,l) = \int f(B)P_0(B;E,l)dB$, where $P_0(B;E,l)$ is the penetration probability of one-dimensional barrier (of height B) at a given center-of-mass energy E and angular momentum l. P_0 may be approximated, for example, by the usual Hill-Wheeler formula [29].

The barrier distribution function $f(B)$, which satisfies the normalization condition $\int f(B)dB = 1$, may be calculated within the consistent CC model [30,31] using experimental properties of low-lying collective excited states of the nuclei. It may be also approximated basing on the multidimensional nucleus-nucleus interaction $V_{12}(r;\vec{\beta}_1,\theta_1,\vec{\beta}_2,\theta_2)$, where $\vec{\beta} = \{\beta_\lambda\}$ are the dynamic deformations of the projectile and target ($\lambda = 2,3,...$) and $\theta_{i=1,2}$ are the orientations of statically deformed nuclei. Such potential energy is shown in Fig. 1 for the case of ^{64}Ni +^{132} Sn interaction taking into account quadrupole dynamic deformations of both nuclei. The surface rigidities were calculated using the values of 1.35 MeV and 4.04 MeV for E_{2+} excited states in ^{64}Ni and ^{132}Sn, correspondingly.

The following expression was proposed in Ref. [32] as the simplest approximation for the barrier distribution function

$$f(B) = N \begin{cases} \exp\left(-\left[\dfrac{B-B_{\rm av}}{\Delta_1}\right]^2\right), & B < B_{\rm av} \\ \exp\left(-\left[\dfrac{B-B_{\rm av}}{\Delta_2}\right]^2\right), & B > B_{\rm av}, \end{cases} \tag{1}$$

where $B_{\rm av} = (B_1 + B_2)/2$. In the case of spherical colliding nuclei B_1 is the height of the barrier at zero dynamic deformation and B_2 is the height of the saddle point ($B_2 = V_{12}(r;\vec{\beta}_1^{\rm sd},\vec{\beta}_2^{\rm sd}) < B_1$) calculated with realistic vibration properties of the nuclei, i.e., with the surface stiffness parameters obtained from the experimental values of the excited vibrational states (see Fig. 1). For statically deformed nuclei B_1 and B_2 are the heights of the Coulomb barriers calculated for the "side-by-side" and "nose-to-nose" orientations, correspondingly. $N(\Delta_1,\Delta_2)$ is the normalization coefficient and $\Delta_2 = (B_1 - B_2)/2$. Experiments and the theoretical analysis show that for heavy nuclear systems the barrier distribution function is usually asymmetric and the value of Δ_1 is, as a rule, less than the value of Δ_2 by 1 or 2 MeV.

Let us now assume that in addition to the intermediate excitations of collective states [already taken into account by the barrier distribution function $f(B)$] an intermediate neutron transfer (neutron rearrangement) may also occur during the fusion process. If such rearrangement takes place at relatively large distances, before nuclei reach the Coulomb barrier (see below), then the incoming flux penetrates the multidimensional barrier in the different neutron transfer channels. Let us denote by $\alpha_k(E,l;Q)$ the probability for the transfer of k neutrons at the center-of-mass energy E and

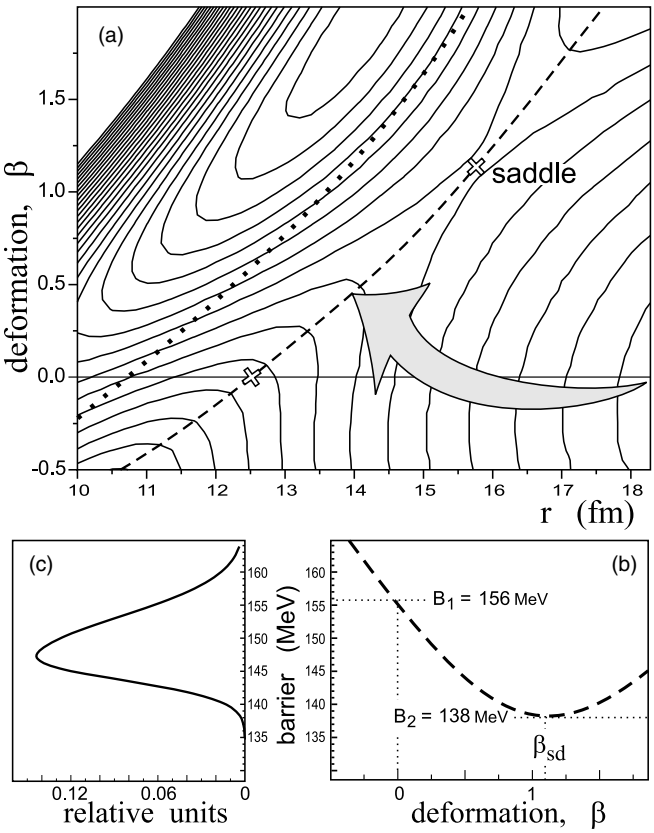

FIG. 1. Potential energy of ^{64}Ni + ^{132}Sn. The proximity potential is used for the nuclear interaction and the surface stiffness parameters are used that reproduce the experimental energies of the 2^+ excited states in the nuclei. (a) Landscape of the potential energy surface. The saddle point and the potential barrier of spherical nuclei ($\beta = 0$) are shown by crosses. The ridge of the barrier is shown by the dashed line, whereas the dotted line corresponds to the contact distance of the two nuclei. The incoming flux is shown schematically by the gray-shaded arrow. (b) Potential energy at the ridge of the two-dimensional barrier, i.e., along the dashed line passing through the saddle point. (c) Empirical barrier distribution function $f(B)$ defined by Eq. (1).

at the relative motion angular momentum l in the entrance channel to the final state with $Q \leqslant Q_0(k)$, where $Q_0(k)$ is a Q value for the ground-state-to-ground-state transfer reaction. Then the total penetration probability may be written as [27]

$$T(E,l) = \int f(B)\frac{1}{N_{\rm tr}}\sum_k \int_{-E}^{Q_0(k)} \alpha_k(E,l;Q) \times P_0(B;E+Q,l)\,dQdB, \qquad (2)$$

where $N_{\rm tr} = [\Sigma_k \int \alpha_k(E,l;Q)dQ]$ is the normalization constant and $\alpha_0 = \delta(Q)$ (fusion without neutron transfer).

In heavy-ion collisions the de Broglie wavelength of relative motion is usually less than the Coulomb barrier distance, R_B. In that case a semiclassical approximation may be used, in principle, to estimate roughly the neutron transfer probability. Assuming predominance of sequential neutron transfer mechanism, which means multiplication of transfer probabilities, one get $\alpha_k(E,l;Q) \sim e^{-2\xi D(E,l)}$, where $D(E,l)$ is the distance of closest approach of the two nuclei and $\xi = \xi(\epsilon_1) + \xi(\epsilon_2) + ... + \xi(\epsilon_k)$ for sequential transfer of k neutrons, $\xi(\epsilon_i) = \sqrt{2\mu_n\epsilon_i/\hbar^2}$ and ϵ_i is the separation energy of the i-th transferred neutron. Experiments show that the transfer probability becomes very close to unity at a short distance between the two nuclei, when their surfaces are well overlapping. We denote this distance by $D_0 = d_0(A_1^{1/3} + A_2^{1/3})$, where the parameter d_0 has the value of about 1.40 fm. In heavy-ion few-neutron transfer reactions the final states with $Q_{\rm opt} \approx 0$ are populated with largest probability due to mismatch of incoming and outgoing waves. The Q window may be approximated by the Gaussian exp $(-C[Q - Q_{\rm opt}]^2)$ with the constant $C = R_B\mu_{12}/(4\hbar^2\xi B)$ [33], where μ_{12} is the reduced mass of the two nuclei. Finally, the transfer probability may be estimated in the following way

$$\alpha_k(E,l;Q) = N_k e^{-C[Q-Q_{\rm opt}]^2} e^{-2\xi[D(E,l)-D_0]}, \qquad (3)$$

where $N_k = \{[\int_{-E}^{Q_0(k)} \exp(-C[Q - Q_{\rm opt}]^2)dQ\}^{-1}$ and the second exponent has to be replaced by 1 for $D(E,l) < D_0$.

Expression similar to Eq. (2) for the transmission probability (taking into account intermediate neutron transfers) was proposed also in Ref. [26]. The neutron transfer probability term $\alpha_k(E,l;Q)$ depending on the incident energy and angular momentum (not only on the Q value) is a distinction in kind between the two models. This term is very important for deep sub-barrier energies when the distance of closest approach $D(E,l)$ is rather large and neutron transfer probability is low. In addition to correct calculation of the effects of neutron transfer on sub-barrier fusion, Eq. (3) may be used also for a reasonable simultaneous description (with the same nucleus-nucleus interaction potential) of the elastic scattering and few neutron transfer angular distributions as well as the total neutron transfer cross sections [27], which, among other things, significantly reduces uncertainty in the values of the used parameters.

From Eq. (2), one can see that in reactions with negative values of all $Q_0(k)$ there is no *additional* enhancement of the total penetration probability of the Coulomb barrier $T(E,l)$ due to the neutron rearrangement, because the "partial" penetration probability $P_0(B;E+Q,l)$ becomes smaller for negative Q values as compared to $Q = 0$. It means that intermediate neutron transfers with zero and/or negative Q values (most probable processes) really take place but cannot enhance the penetration probability. If, however, $Q_0(k)$ are positive for some channels, in spite of the lower transfer probability to the states with positive Q values as compared to $Q = 0$, the total penetration probability may significantly increase due to a gain in the relative motion energy in the channels with $Q > 0$. In other words, an intermediate neutron transfer to the states with $Q > 0$ is, in a certain sense, an "energy lift" for the two interacting nuclei.

At first sight, this interpretation looks quite different from the well-known fusion enhancement due to surface vibrations or rotation of nuclei leading to decrease of potential barrier in some channels. However, if we consider the potential energy of the two interacting nuclei as a function of a number of transferred neutrons, $V_{12}(r;\Delta N)$ (in addition to other

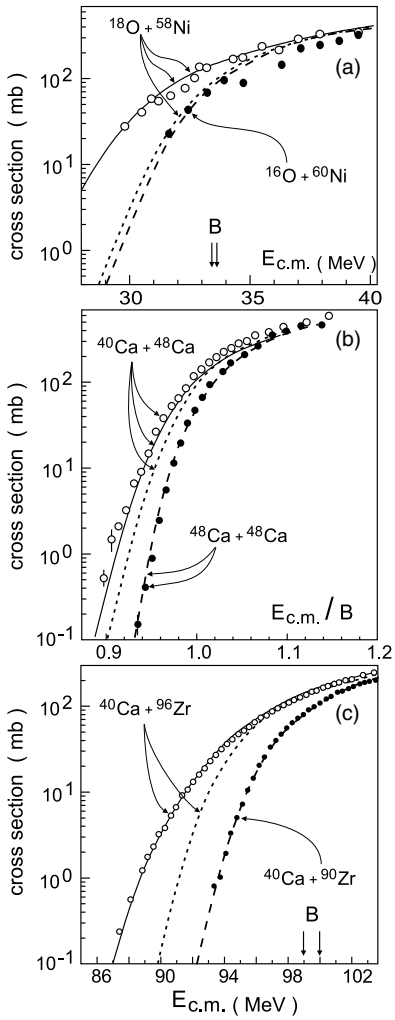

FIG. 2. Fusion cross sections for $^{16}O + ^{60}Ni$ and $^{18}O + ^{58}Ni$ [14] (a), $^{40}Ca + ^{48}Ca$ and $^{48}Ca + ^{48}Ca$ [12] (b), $^{40}Ca + ^{90}Zr$ and $^{40}Ca + ^{96}Zr$ [15] (c). Dashed curves are the CC calculations for the $^{16}O + ^{60}Ni$, $^{48}Ca + ^{48}Ca$, and $^{40}Ca + ^{90}Zr$ fusion reactions. Dotted curves are the CC calculations for the $^{18}O + ^{58}Ni$, $^{40}Ca + ^{48}Ca$, and $^{40}Ca + ^{96}Zr$ fusion reactions, whereas the solid curves are the results of calculations for the same reactions in accordance with formula (2), i.e., taking into account intermediate neutron rearrangement.

variables), then we will find that the height of the Coulomb barrier for some $\Delta N \neq 0$ is lower than in the entrance channel ($\Delta N = 0$) for those nuclear combinations in which neutron transfer with positive Q value is possible. Thus, we may also interpret this effect in the usual way as a lowering of the Coulomb barrier due to the channel coupling (see also the next section).

In Fig. 2 the sub-barrier fusion cross sections are shown for different combinations of colliding nuclei: $^{18}O + ^{58}Ni$ ($Q_0(1n) = +0.96$ MeV, $Q_0(2n) = +8.2$ MeV) compared with $^{16}O + ^{60}Ni$ (all $Q_0(k) < 0$), $^{40}Ca + ^{48}Ca$ ($Q_0(2n) = +2.6$ MeV, $Q_0(4n) = +3.9$ MeV) compared with $^{48}Ca + ^{48}Ca$ (all $Q_0(k) < 0$), and $^{40}Ca + ^{96}Zr$ ($Q_0(1n) = +0.5$ MeV, $Q_0(2n) = +5.5$ MeV, $Q_0(3n) = +5.2$ MeV, $Q_0(4n) = +9.6$ MeV) compared with $^{40}Ca + ^{90}Zr$ (all $Q_0(k) < 0$). One can see that the sub-barrier fusion probabilities are much higher for the combinations of nuclei where a rearrangement of neutrons with positive Q values is possible. Moreover, for such combinations the standard CC approach cannot properly describe experimental data by any reasonable variation of parameters, whereas for other combinations this method demonstrates very nice agreement with experiment. Additional fusion enhancement here is reproduced quite well if we assume the intermediate rearrangement of valence neutrons and apply Eqs. (2) and (3) for a calculation of the cross sections (see Fig. 2). Significant sub-barrier fusion enhancement was found recently also for the $^{40}Ca + ^{94}Zr$ combination [34] (similar to $^{40}Ca + ^{96}Zr$) in which an intermediate neutron transfer (up to four neutrons) with positive Q values is possible too.

As mentioned above, the neutron excess (leading normally to the lowering of the Coulomb barrier due to increase of the nuclear radius) does not lead obligatory to additional sub-barrier fusion enhancement. It was confirmed recently in the experiment on fusion of extremely neutron rich nuclei [10]. The enhancement in the $^{64}Ni + ^{132}Sn$ fusion reaction relative to lighter Sn isotopes was found to be not larger than would be expected due to the larger nuclear radius of ^{132}Sn and, thus, neutron transfer does not appear to play a major role in the sub-barrier fusion for this system. ^{132}Sn is really not so much different from ^{124}Sn. Two-neutron separation energies differ by less than 2 MeV for these nuclei. In this connection, we may expect a noticeable sub-barrier fusion enhancement only for the $^{64}Ni + ^{134}Sn$ combination, in which neutron transfers with rather large positive Q values ($Q_0(1n) = 2.35$ MeV, $Q_0(2n) = 8.9$ MeV) are possible (obviously, the effect should be even larger for the $^{58}Ni + ^{134}Sn$ combination).

In Fig. 3 the cross sections for the $^{64}Ni + ^{132}Sn$ and $^{64}Ni + ^{134}Sn$ fusion reactions are shown calculated with and without intermediate neutron rearrangement. A proximity potential [35] (giving the barriers of 155.8 and 155.4 MeV,

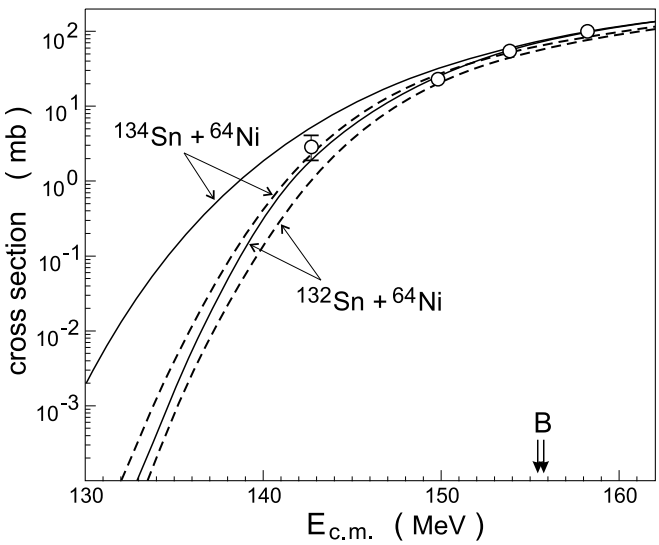

FIG. 3. Fusion cross sections for $^{132}Sn + ^{64}Ni$ and $^{134}Sn + ^{64}Ni$ calculated with (solid curves) and without (dashed curves) intermediate neutron rearrangement. Experimental data for $^{132}Sn + ^{64}Ni$ are taken from Ref. [1].

correspondingly) was used to calculate the barrier penetrability $P_0(B; E, l)$ in Eq. (2), and the experimental energies of the 2^+-excitations in ^{64}Ni and ^{132}Sn were used to find the barrier distribution function $f(B)$ (see Fig. 1). As can be seen, the neutron rearrangement significantly increases the sub-barrier fusion cross section only for the ^{64}Ni + ^{134}Sn combination and plays a minor role for the ^{64}Ni + ^{132}Sn fusion reaction.

It is clear that a much stronger effect from the neutron transfer with positive Q values can be expected in fusion of light neutron-rich weakly bound projectiles with stable targets. To avoid additional ambiguities (see above) one may propose to measure the evaporation residue (EvR) cross sections for reactions, in which the same compound nucleus is formed, such as ^{6}He + $^A X \rightarrow$ CN and ^{4}He + $^{A-2}X \rightarrow$ CN, for example. In that case any difference in the EvR cross sections may originate only from the difference in the entrance channels of the two reactions. The promising reactions of such type are ^{6}He + ^{206}Pb and ^{4}He + ^{208}Pb with the formation of α-decayed $^{212-xn}$Po compound nuclei. In the first combination there are intermediate neutron transfer channels with very large positive Q values: ^{6}He + ^{206}Pb $\rightarrow$ ^{5}He + ^{207}Pb(Q_0 = 4.9 MeV) $\rightarrow$ ^{4}He + ^{208}Pb(Q_0 = 13.1 MeV) $\rightarrow$ ^{212}Po. Of course, as mentioned above, the probability for neutron transfer to the ground states is rather small, but the total possible gain in energy is very large here as compared with the height of the Coulomb barrier (which is about 20 MeV) and has to reveal itself in the fusion probability of ^{6}He compared to ^{4}He.

A schematic picture of the described "sequential fusion" mechanism in sub-barrier collision of ^{6}He with ^{206}Pb is shown in Fig. 4 taken from [36]. When the colliding nuclei approach, two valence neutrons may be transferred from ^{6}He to the ground and low-lying states of ^{208}Pb with a small, but not negligible probability. In that case, the charged core finds itself with kinetic energy well above the Coulomb barrier and may easily fuse with the target. Coupling to the continuum states of weakly bound ^{6}He nucleus could be also very important (due to a large break-up cross section for ^{6}He in collisions with heavy targets [37]), and it is not taken into account by Eq. (2). However recent calculations performed within the CDCC model [23] show that the coupling to the continuum influences the near-barrier fusion cross section (increasing it) with a factor less than 1.5.

The experiment on fusion of ^{6}He with ^{206}Pb target was proposed first in Ref. [27], where the yield of Po isotopes was predicted several orders of magnitude (!) higher as compared with the ^{4}He + ^{208}Pb fusion reaction (see Fig. 5). Recently at the Joint Institute for Nuclear Research (Dubna)

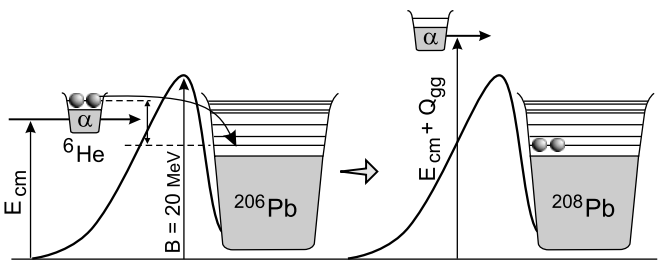

FIG. 4. Schematic picture of sequential fusion of ^{6}He.

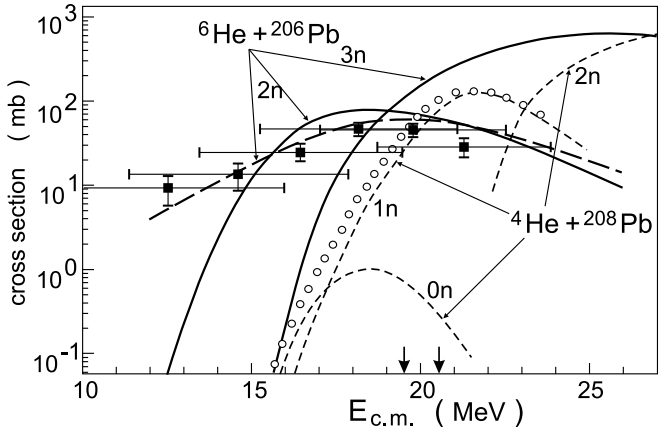

FIG. 5. Cross sections for the production of Po isotopes in the ^{6}He+^{206}Pb (solid curves) and ^{4}He+^{208}Pb (short dashed curves) fusion reactions calculated in Ref. [27]. Open circles show experimental yield of ^{211}Po in the ^{4}He + ^{208} Pb fusion reaction [38] ($1n$ channel). Solid squares are the cross sections for production of ^{210}Po in the ^{6}He + ^{206} Pb fusion reaction ($2n$ channel) measured recently in Dubna [7]. Long-dashed curve includes the effect of the energy spread of the ^{6}He beam for the calculated $2n$-channel cross sections. Arrows at the energy axis show the corresponding Coulomb barriers for ^{6}He (left) and ^{4}He (right) which are very close to each other.

the corresponding experiment has been performed [7] that completely confirmed our expectations. The activation method was used in this experiment in which a stack of six ^{206}Pb targets, each 600–700 μg/cm^2 thick, with 20-μm Al foils inserted in between to reduce the beam energy from 23 to 13 MeV. It was irradiated with the ^{6}He beam giving the six data points shown in Fig. 5. Unfortunately this method gives rather large energy spread of the ^{6}He beam inside the target. As can be seen from Fig. 5, at sub-barrier energies the fusion cross section is falling exponentially and the energy spread may distort significantly the experimental data. To estimate this effect we averaged the calculated cross sections for the $2n$-channel over the beam width assuming a gaussian distribution with the width of 3 MeV. The result is shown by the long-dashed curve in Fig. 5. Indeed, at the beam energy of 12.5 MeV this effect increases the cross section almost by two orders of magnitude. Thus, new experiments are very desirable to measure the fusion cross sections in this region more accurately. However, as can be seen from the figure, at deep sub-barrier energies the bare fusion probability of ^{6}He with lead target is definitely much larger (about 1000 times at 15 MeV) as compared to the fusion of ^{4}He.

Quite recently the cross section for the fusion of ^{9}Li with ^{70}Zn was measured at near and sub-barrier energies [39]. The observed fusion excitation function shows significant sub-barrier fusion enhancement which can not be described within the standard CC calculations. Neutron rearrangement with positive Q values—^{9}Li + ^{70}Zn $\rightarrow$ ^{8}Li + ^{71}Zn(Q_0 = 1.77 MeV) $\rightarrow$ ^{7}Li + ^{72}Zn(Q_0 = 8.62 MeV)—is possible for this reaction which may significantly increase the sub-barrier fusion probability. We performed an analysis of this reaction using the same nucleus-nucleus potential as in Ref. [39] (Woods-Saxon type potential with $V_0 = -105$ MeV, $r_0 =$

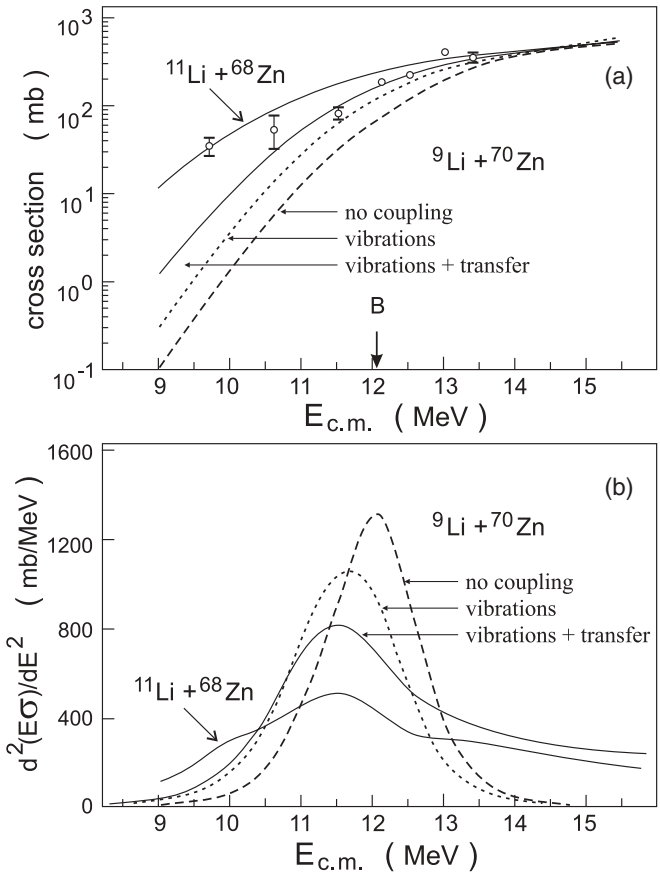

FIG. 6. Fusion cross sections (a) and barrier distribution function, $d^2(E\sigma)/dE^2$ (b) for the fusion reactions ^{9}Li + ^{70}Zn and ^{11}Li + ^{68}Zn. Experimental data are for the ^{9}Li + ^{70} Zn fusion reaction taken from Ref. [39].

1.12 fm, $a = 0.65$ fm). One-dimensional barrier penetration model gives the result shown in Fig. 6 by the dashed curves. Assuming that the lowest excitation energies in ^{9}Li (2.6 MeV) and ^{70}Zn (0.88 MeV) correspond to the quadrupole vibrations of these nuclei we calculated the effect of coupling with surface vibrations which is shown in Fig. 6 by the dotted curves. This effect is really not so much and cannot explain the observed fusion enhancement. Then we took into account the effect of neutron rearrangement as described above. Intermediate neutron transfer noticeably increases the sub-barrier fusion probability but still insufficient to describe the deep sub-barrier fusion cross section found in the experiment (see Fig. 6). It could be due to more probable "di-neutron" transfer as compared to the sequential neutron transfer used for the calculation of the ^{9}Li + ^{70}Zn fusion cross section.

Anyhow, fixing all the parameters, we calculated also the cross section for the ^{11}Li + ^{68}Zn fusion reaction leading to the same compound nucleus and, thus, to the same evaporation residues. Two-neutron separation energy for ^{11}Li is only 0.3 MeV and the Q value is extremely large for the transfer of two neutrons to the ground state of ^{70}Zn, $Q_0(2n) = 15.4$ MeV. As a result the sub-barrier fusion cross section for this reaction should be also significantly larger as compared to ^{9}Li + ^{70}Zn. Because ^{10}Li is an unbound nucleus, we assumed here for the two-neutron rearrangement channel a simultaneous transfer of "di-neutron" with the corresponding separation energy $\epsilon_{2n} = 0.3$ MeV. The obtained result is shown in Fig. 6. Obviously the sub-barrier fusion probability for ^{11}Li is much larger than for ^{9}Li. Note that the coupling to the breakup channel may slightly decrease the fusion cross section for ^{11}Li at above and near-barrier energies. Thus, direct experimental comparison of the yields of the evaporation residues in both reactions at sub-barrier energies is of great interest.

III. MICROSCOPIC ANALYSIS

In spite of rather good agreement with experimental data of the cross sections obtained within the semiempirical approach of "sequential fusion" with intermediate neutron rearrangement [27], we need to study this problem more carefully on a microscopic basis to understand better the role of valence neutrons in fusion processes (also to check the validity of the semiempirical method which may be easily used for estimations of the fusion cross sections). For that we studied the process of sub-barrier fusion of atomic nuclei within a three-body quantum model (two fusing nuclear cores plus a valence neutron) solving the time-dependent Schrödinger equation. We tried to find clear answers on the two questions: (1) What happens with the valence neutrons when nuclei approach each other? (2) What is the mechanism of the fusion enhancement due to rearrangement of valence neutrons?

Note that a choice of the Jacobi coordinates for numerical solution of the three-body time dependent Schrödinger equation is important. In Fig. 7 two sets of the Jacobi coordinates are shown. Numerical calculations show that the first set of the Jacobi coordinate $(\vec{\rho}_{2(13)}, \vec{\rho}_{13})$ is quite appropriate for description of the breakup process. However there is a bad convergence of the results (over the partial waves of relative motion of neutron and target nucleus) if one uses this system of coordinate for the description of neutron transfer and fusion processes. We found that the two-center Jacobi coordinates $(\mathbf{r}, \mathbf{R})$ are most appropriate to describe neutron rearrangement and fusion.

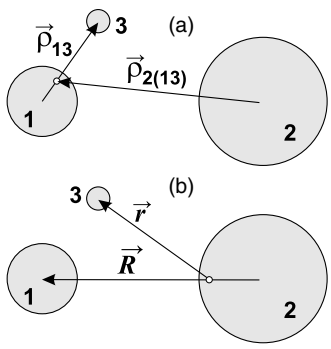

FIG. 7. Jacobi coordinates optimal for description of the system consisting of two cores and a valence neutron at large (a) and short (b) distances between the two cores.

To answer the first question we solved numerically the time-dependent Schrödinger equation

$$i\hbar\frac{\partial\Psi}{\partial t} = \left[-\frac{\hbar^2}{2m_3}\Delta_{\mathbf{r}_3} + V_n(\mathbf{r}_3;\mathbf{r}_1(t),\mathbf{r}_2(t))\right]\Psi(\mathbf{r}_3,t), \quad (4)$$

to investigate the evolution of the valence neutron's wave function $\Psi(\mathbf{r}_3,t)$ in the field of the two heavy cores ($m_1, m_2 \gg m_3$) moving along the classical trajectories $\mathbf{r}_1(t)$ and $\mathbf{r}_2(t)$ in the field of $V_{12}(R) = V_C(R) + V_N(R)$ (for nuclear part of this interaction we used the proximity potential [35]). At $R \geqslant R_{\rm cont} = R_1 + R_2$ the neutron potential energy is defined as $V_n(\mathbf{r}_3;\mathbf{r}_1,\mathbf{r}_2) = V_{13}(|\mathbf{r}_3-\mathbf{r}_1|) + V_{23}(|\mathbf{r}_3-\mathbf{r}_2|)$. After fusion $V_n \to V_{\rm CN}(|\mathbf{r}_3-\mathbf{r}_{\rm CN}|)$. We define the model potential by the linear interpolation

$$V_n(\mathbf{r}_3;\mathbf{r}_1,\mathbf{r}_2) = (1-\xi)V_{\rm CN}(|\mathbf{r}_3-\mathbf{r}_{\rm CN}|) + \xi[V_{13}(|\mathbf{r}_3-\mathbf{r}_1|) + V_{23}(|\mathbf{r}_3-\mathbf{r}_2|)], \quad (5)$$

where $\xi = 1$ at $R \geqslant R_{\rm cont}$, $\xi = 0$ at $0 \leqslant R \leqslant R_{\rm int}$, $\xi = (R-R_{\rm int})/(R_{\rm cont}-R_{\rm int})$ otherwise and $R_{\rm int} = |R_1 - R_2|$. Note that we solved the Schrödinger equation up to nuclei come in contact. However, we defined the potential energy in the whole space to avoid some nonphysical reflection effects in behavior of the neutron wave function $\Psi(\mathbf{r}_3,t)$.

Aiming mainly on a qualitative understanding of the process we disregarded spin of the neutron. For the neutron-core interactions we used the model Woods-Saxon type potentials

$$V_{i3}(r) = -V_{0i}\{1+\exp[(r-R_i)/a]\}^{-1} + \Delta V_i(r), i = 1,2 \quad (6)$$

with the small short-range repulsion $\Delta V(r) = \Delta V_0 e^{-(r/b)^2}$ allowing one to reproduce somehow the realistic positions of the single-particle states in the Fermi energy region. The following parameters have been used in calculations: $V_0 = 63\,\text{MeV}$, $r_0 = 1.2$ fm, $a = 0.65$ fm, $\Delta V_0 = 5\,\text{MeV}$, $b = 3$ fm for ^{40}Ca and $V_0 = 59.5\,\text{MeV}$, $r_0 = 1.15$ fm, $a = 0.65$ fm, $\Delta V_0 = 6.7\,\text{MeV}$, $b = 3$ fm for ^{96}Zr. This potential energy is shown in Fig. 8 depending on the internuclear distance.

Numerical solution of Eq. (4) is started at $t = 0$ with the initial conditions $\mathbf{r}_1(t=0)$, $\mathbf{v}_1 = \dot{\mathbf{r}}_1(t=0)$, $\mathbf{r}_2(t=0)$, $\mathbf{v}_2 = \dot{\mathbf{r}}_2(t=0)$ for heavy cores located at a large distance from each other, $|\mathbf{r}_1(0) - \mathbf{r}_2(0)| = R_m \sim 50$ fm, where the nuclear interaction is negligible. For the neutron wave function we chose the initial condition corresponding to its bound state in one of the fragments $\Psi(\mathbf{r}_3, t=0) = \exp[im_3\mathbf{v}_j(0)\mathbf{r}_3/\hbar]\varphi_{nlm}[\mathbf{r}_3 - \mathbf{r}_j(0)]$, $j = 1, 2$. For the Coulomb interaction the values of $\mathbf{r}_1(0)$, $\mathbf{v}_1(0)$, $\mathbf{r}_2(0)$, $\mathbf{v}_2(0)$ can be found in analytical form for a given impact parameter and initial center-of-mass energy of collision [40].

Due to axial symmetry of the potential energy $V_n(\rho,z;R)$ the quasimolecular single particle states may be written as $\Phi_{\alpha\lambda}(\rho,z,\varphi;R) = f_{\alpha\lambda}(\rho,z;R)\exp(\pm i\lambda\varphi)$ (where $\lambda = |m|$ is the projection of the angular momentum on the internuclear axis), and the functions $f_{\alpha\lambda}$ satisfy the equation

$$-\frac{\hbar^2}{2m_3}\left[\frac{\partial}{\rho\partial\rho}\left(\rho\frac{\partial}{\partial\rho}\right) + \frac{\partial^2}{\partial z^2}\right]f_{\alpha\lambda} + \left[V_n(\rho,z;R) + \frac{\hbar^2\lambda^2}{2m_3\rho^2}\right]f_{\alpha\lambda} = \varepsilon_{\alpha\lambda}f_{\alpha\lambda}(\rho,z;R), \quad (7)$$

which may be solved numerically (see details in Ref. [41]). Centrifugal potential $\hbar^2\lambda^2/2m_3\rho^2$ in Eq. (7) hinders neutron tunneling through the narrow manhole along internuclear axis (small values of ρ). Thus the neutron transfer decreases with increasing λ and we found that it is most probable just at $\lambda = 0$.

The two-center single-particle neutron levels $\varepsilon_{\alpha\lambda}(R)$ (quasimolecular states) are shown in Fig. 9 for collision of ^{96}Zr with ^{40}Ca. At deep penetration of the nuclei ($R \ll R_{\rm cont}$) $\varepsilon_{\alpha,\lambda}(R)$ increases due to a small decrease of the nuclear volume (we do not care of it here). Of course, it does not occur at slow near-barrier collisions when the nucleons have enough time to reach equilibrium distribution and the shape of mono-nucleus satisfies to volume conservation (adiabatic condition). However, for our calculations it is not important because we do not consider evolution of the system after nuclei come in contact.

We did not decompose the total wave function $\Psi(\mathbf{r}_3,t)$ over the molecular states and used them only for analysis of the obtained results (see below). The time-dependent Schrödinger

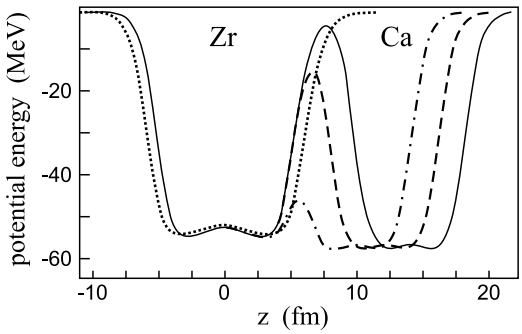

FIG. 8. Neutron potential energy in the ^{40}Ca $+^{96}$ Zr system along the internuclear axis at different distances $R = 14$ fm, $R = 12$ fm, $R = 10$ fm, and $R = 1$ fm (solid, dashed, dot-dashed, and dotted curves, respectively).

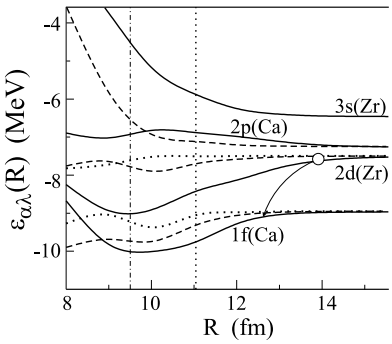

FIG. 9. Two-center quasimolecular single particle neutron levels in the ^{96}Zr $+^{40}$Ca nuclear system. Solid, dashed, and dotted curves show the states with $\lambda = 0, 1$, and 2, respectively. $2d$ is the last occupied level in ^{96}Zr; $1f$ and $2p$ are unoccupied levels of ^{40}Ca. Vertical dotted and dash-dotted lines show positions of the Coulomb barrier and the contact point, correspondingly.

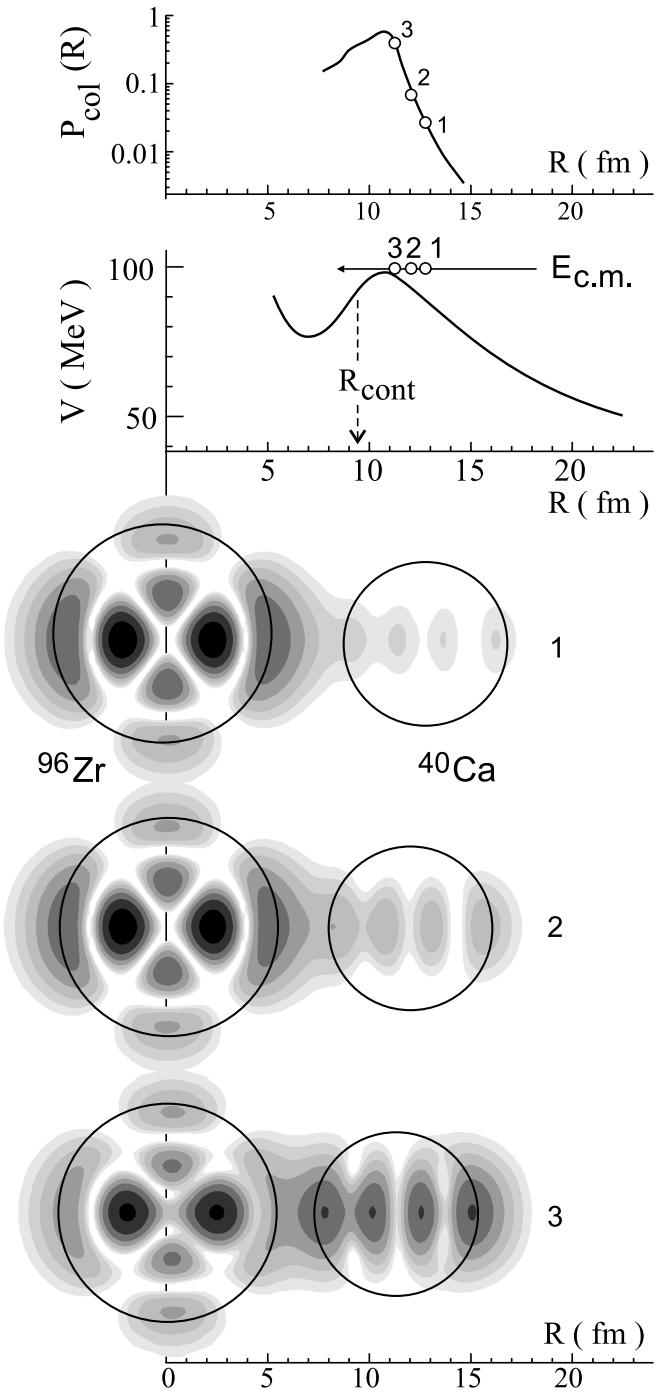

FIG. 10. Amplitude of the wave function of valence neutron (initially located in the $2d$ state of ^{96}Zr nucleus) at the three distances between colliding nuclei shown by the small circles in the upper part of the figure along with the probability to find the neutron in the ^{40}Ca nucleus.

equation (4) was solved directly using the finite difference scheme proposed in Ref. [42] coupled with the fast Fourier transformation. In Fig. 10 the probability density $|\Psi(\mathbf{r}_3, t)|^2$ is shown for the valence neutron initially located in the $2d$ state of ^{96}Zr approaching a ^{40}Ca nucleus in a head-on collision at near-barrier center-of-mass energy $E = 97$ MeV.

Using this wave function we may estimate a rate of neutron collectivization, that is a probability to find the valence neutron into the volume of the nucleus-acceptor (note that this is not a real transfer probability that has to be determined for well-reseparated nuclei). Such probability can be calculated by an integration of the wave function over the volume of the acceptor nucleus

$$P_{\rm col}(t) = \int_{\omega} |\Psi(\mathbf{r}_3, t)|^2 d^3\mathbf{r}_3, \tag{8}$$

where the volume $\omega \equiv \{z_1 - z_3 < (R + R_1 - R_2)/2, |\mathbf{r}_3 - \mathbf{r}_1| < R_1 + \Delta r\}$, $\mathbf{R} = \mathbf{r}_1 - \mathbf{r}_2$, $\Delta r \sim 2$ fm and $R_{1,2}$ are the radii of the colliding nuclei. Dependence of the neutron collectivization on the distance between the two nuclei is shown in upper part of Fig. 10. Thus, we may conclude that spreading of the valence neutron's wave function into the volume of the other nucleus takes place before touching of these nuclei and even before the colliding nuclei overcome the Coulomb barrier. Among other things this supports the idea of "sequential fusion" mechanism [27] discussed above.

Within the used model the two factors may significantly enhance the fusion probability due to a neutron rearrangement. First, at the barrier region some of the occupied levels may decrease an energy (see Fig. 9) and, consequently, decrease the channel adiabatic potential energy $V_{\alpha\alpha}(R) = V_{12}(R) + \varepsilon_\alpha(R) - \varepsilon_\alpha(\infty)$. Second, the transfer of the valence neutron from its initial state α to unoccupied state β also changes the channel potential energy: $V_{\alpha\beta}(R) = V_{12}(R) + \varepsilon_\beta(R) - \varepsilon_\alpha(\infty)$. The corresponding occupation probability of a given quasimolecular state, p_α, may be estimated as a projection of the total wave function onto the quasimolecular single-particle state Φ_α

$$p_\alpha(t) = \left| \int \Phi^*_\alpha(\mathbf{r}_3, R(t)) \Psi(\mathbf{r}_3, t) d^3\mathbf{r}_3 \right|^2. \tag{9}$$

Thus, the total effective potential energy $\sim \Sigma_\beta V_{\alpha\beta}(R) p_\beta(R)$ may significantly differ from the initial potential with "frozen" neutrons, $V_{12}(R)$, see Fig. 11. This may lead to an enhancement of the sub-barrier fusion probability and also to a nonuniform energy dependence of the penetration probability (the result of several channel barriers). Of course this is a qualitative explanation because so far we used a classical motion for the variable R. It should be noted also that not included in the model residual nucleon-nucleon interactions may significantly increase the probability of the neutron transfer to unoccupied low-lying states.

To answer the second question one has to consider a full three-body quantum model (including quantum motion and tunneling along the variable R). For simplicity we solved numerically the three-body one-dimensional time dependent Schrödinger equation (keeping in mind a head-on collisions at sub-barrier energies at which the valence neutron only moves in one dimension along the internuclear axis)

$$i\hbar \frac{\partial}{\partial t} \Psi(r, R, t) = \left[-\frac{\hbar^2}{2\mu} \frac{\partial^2}{\partial r^2} - \frac{\hbar^2}{2M} \frac{\partial^2}{\partial R^2} + V_{12}(R) + V_n(r, R) \right] \Psi(r, R, t), \tag{10}$$

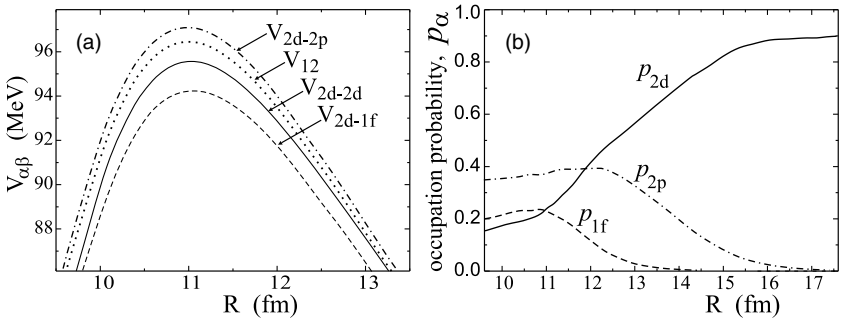

FIG. 11. Channel nucleus-nucleus interactions (a) and quasimolecular occupation probabilities (b) for collision of ^{96}Zr and ^{40}Ca at $E_{\text{c.m.}} = 97$ MeV: initial interaction V_{12} (dotted curve), $V_{2d,2d}$ and the corresponding occupation probability p_{2d} (solid curves), $V_{2d,1f}$ and p_{1f} (dashed curves), $V_{2d,2p}$ and p_{2p} (dot-dashed curves).

where $r = r_3 - (m_1 r_1 + m_2 r_2)/(m_1 + m_2)$ is the distance of the valence neutron from the center of mass of two colliding nuclei, $r_1 = R\eta_1 - r\eta_2, r_2 = R(\eta_1 - 1) - r\eta_2, r_3 = r(1 - \eta_2), \eta_1 = m_2/(m_1 + m_2), \eta_2 = m_3/(m_1 + m_2 + m_3), 1/\mu = 1/m_3 + 1/(m_1 + m_2), 1/M = 1/m_1 + 1/m_2$, see Fig. 7. In contrast with Eq. (4), here we use the reduced masses for relative motions meaning in future to apply Eq. (10) also for description of sub-barrier fusion of not so heavy ions.

The initial condition for the solution of Eq. (10) consists of the neutron bound wave function and the wave packet of relative motion located at some large distance R_m

$$\Psi(r, R, t = 0) = C\varphi_n(r_3 - r_2)h_0^{(-)}(r_A - r_1) \times \exp\left[-\frac{(r_A - r_1 - R_m)^2}{2a_p^2}\right], \quad (11)$$

where $r_A = (m_2 r_2 + m_3 r_3)/(m_2 + m_3), h_0^{(-)}(r) = G_0(r) - iF_0(r)$, G_0, F_0 are the Coulomb wave functions and for the width of the wave packet, a_p, we used the value of 5 fm.

Equation (10) was also solved with the finite difference scheme proposed in Ref. [42] coupled with the fast Fourier transformation. This gives rather high absolute accuracy ($\sim 10^{-4}$) and allows one to study the deep sub-barrier fusion processes. Amplitude of the time-dependent wave function $\Psi(r, R, t)$ is shown in Fig. 12 for the sub-barrier collision of ^{40}Ca with ^{96}Zr. Neutron transfer from ^{96}Zr to the lower-lying state in ^{40}Ca splits the wave packet over the R variable (relative motion of the nuclei). The part of the wave packet with the neutron localized in ^{40}Ca finds itself closer to the barrier (due to a gain in kinetic energy) and overcomes the barrier with higher probability.

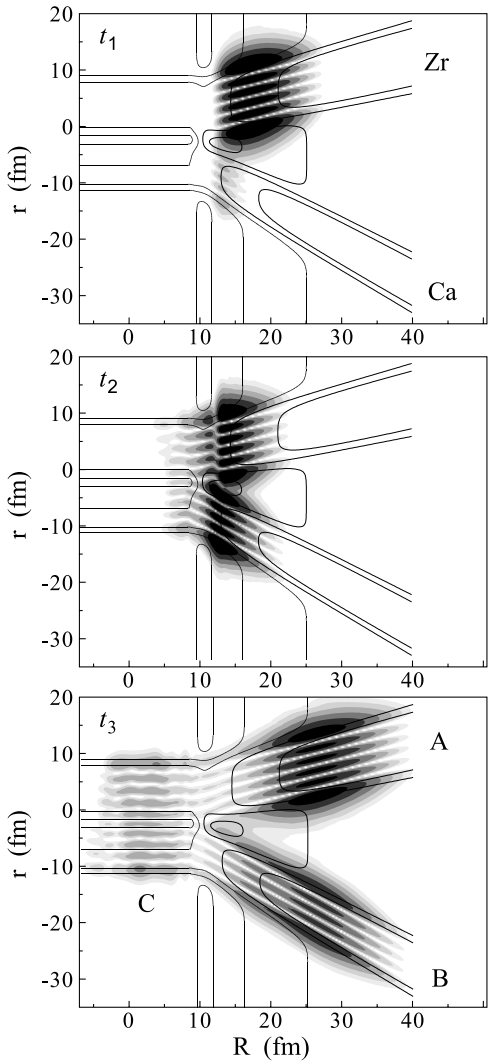

FIG. 12. Probability density $|\Psi(r, R, t)|^2$ for collision of ^{40}Ca with ^{96}Zr at sub-barrier energy $E = B - 10 = 90$ MeV in the one-dimentional quantum model. Solid curves show equipotential levels for the potential energy $V_{12}(R) + V_n(r; R)$. $t_1 = 10^{-21}$s, $t_2 = 2 \times 10^{-21}$s, $t_3 = 3 \times 10^{-21}$s. Regions A, B, and C correspond to the scattering (neutron remains in Zr nucleus), transfer and fusion processes, correspondingly.

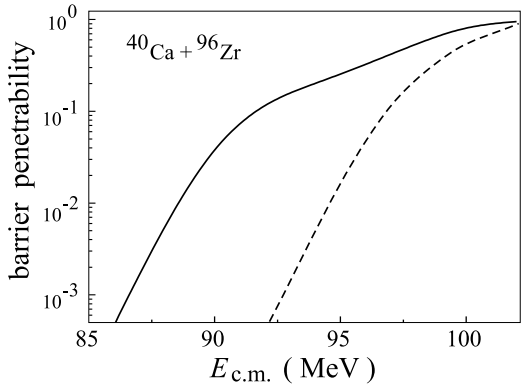

FIG. 13. Barrier penetrability for collision of ^{40}Ca with ^{96}Zr calculated in the three-body one-dimensional model. The dashed curve shows the result obtained for "frozen" neutron (penetration probability of one-dimensional barrier $V_{12}(R)$).

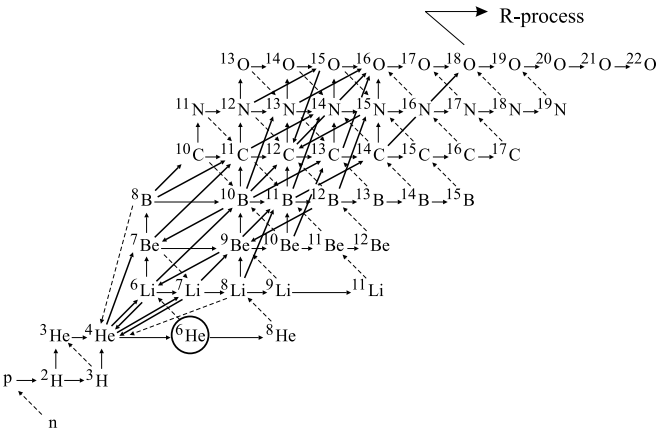

FIG. 14. Part of the nuclear reaction network usually used for the calculations [43].

For a normalized initial condition the barrier penetration probability at the moment t is equal to the total flux overcoming the barrier at $R = R_B$

$$T(t, E) = \int_{-\infty}^{t} J(t')dt', \quad J(t) = -\int_{-\infty}^{\infty} j_R(r, R_B, t)dr,$$
$$j_R = \frac{\hbar}{M}\mathrm{Im}\left\{\Psi^* \frac{\partial}{\partial R}\Psi\right\}. \qquad (12)$$

The total penetration probability is defined as $T(E) = \lim T(t, E)|_{t\to\infty}$. The barrier penetration probability calculated within the one-dimensional three-body model for the ^{48}Ca + ^{96}Zr fusion reaction is shown in Fig. 13.

Both factors, the lowering of the initially occupied valence neutron level in ^{96}Zr and the possibility for neutron transfer into the unoccupied lower lying state in ^{40}Ca, play significant role and considerably enhance the sub-barrier fusion of ^{40}Ca with ^{96}Zr. Note that for the ^{96}Zr + ^{48}Ca nuclear system none of these factors applies: $1f\frac{7}{2}$ level in ^{48}Ca is fully occupied and this is the reason that the energy of the $2d\frac{5}{2}$ state in ^{96}Zr does not decrease when these nuclei approach each other. Thus we may definitely conclude that this is a possibility for a "positive Q value" neutron transfer (existence of unoccupied lower lying levels) that leads to the sub-barrier fusion enhancement due to the two factors, namely, lowering of the valence quasimolecular state in one nucleus (usually more neutron rich) and neutron transfer from this state to the lower (unoccupied) state of the other nucleus.

IV. ASTROPHYSICAL ASPECTS

The sub-barrier fusion enhancement for weakly bound neutron rich nuclei can be used, in principle, for the synthesis of new superheavy nuclei in future experiments with accelerated fission fragments. The enhancement effect in deep sub-barrier

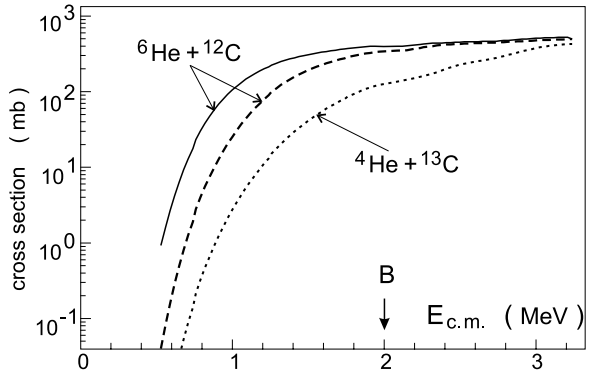

FIG. 15. Near barrier cross sections for the ^{6}He + ^{12}C (dashed curve assumes sequential neutron transfer whereas solid curve takes into account $2n$ transfer) and ^{4}He+^{13}C (dotted curve) fusion reactions.

fusion probability of light weakly bound nuclei may be even more important for astrophysical processes. In the standard scenario for the primordial nucleosynthesis (see Fig. 14) the unstable weakly bound nuclei (such as ^{6,8}He, ^{8,9,11}Li and so on) are intensively produced via (n, γ) reactions with subsequent β decay to the stable nuclei (see, e.g., Ref. [43] and references therein). At the same time the fusion reactions like ^{14}C(^{4}He, γ) ^{18}O play very important role in the nucleosynthesis network used for calculation of heavy-element production [44].

From the analysis performed above we may predict that the probability for fusion of light weakly bound neutron rich nuclei with stable nuclei at deep sub-barrier energies should be much higher (probably by several orders of magnitude) as compared to fusion of ordinary nuclei. For example, an estimated cross section for the ^{12}C + ^{6}He fusion reaction at 1 MeV center-of-mass energy ($1n$ and $2n$ open channels), shown in Fig. 15, exceeds by almost two orders of magnitude the cross section for the nonresonance ^{13}C(^{4}He, $n\gamma$) ^{16}O reaction. This is due to neutron rearrangement which gives extremely large gain in energy for the first reaction. The same obviously holds for the corresponding astrophysical S factors. Note that a similar mechanism of neutron rearrangement may also significantly increases the fusion probability of very light nuclei like ^{6}He + ^{3}He. If this prediction will be confirmed experimentally, then the standard scenarios of the primordial and, probably, supernova nucleosynthesis have to be revised to a great extent. Fusion processes of light neutron rich radioactive nuclei, formed with a large probability due to intense neutron flux, may dominate here and have to be included in the whole nucleosynthesis network (at the same level as it is done for ^{3}H, for example). For a final conclusion one needs to know the corresponding S factors that should be measured experimentally. Among other things, this opens exciting future trends for low-energy studies of nuclear reactions with radioactive beams.

[1] J. F. Liang, D. Shapira, C. J. Gross, J. R. Beene, J. D. Bierman, A. Galindo-Uribarri, J. Gomez del Campo, P. A. Hausladen, Y. Larochelle, W. Loveland, P. E. Mueller, D. Peterson, D. C. Radford, D. W. Stracener, and R. L. Varner, Phys. Rev. Lett. **91**, 152701 (2003).
[2] A. S. Fomichev, I. David, Z. Dlouhy, S. M. Lukyanov,

Yu. Ts. Oganessian, Yu. E. Penionzhkevich, V. P. Perelygin, N. K. Skobelev, O. B. Tarasov, and R. Wolski, Z. Phys. A **351**, 129 (1995).
[3] J. J. Kolata, V. Guimarães, D. Peterson, P. Santi, R. White-Stevens, P. A. De Young, G. F. Peaslee, B. Hughey, B. Atalla, M. Kern, P. L. Jolivette, J. A. Zimmerman, M. Y. Lee, F. D. Becchetti, E. F. Aguilera, E. Martinez-Quiroz, and J. D. Hinnefeld, Phys. Rev. Lett. **81**, 4580 (1998).
[4] M. Trotta, J. L. Sida, N. Alamanos, A. Andreyev, F. Auger, D. L. Balabanski, C. Borcea, N. Coulier, A. Drouart, D. J. C. Durand, G. Georgiev, A. Gillibert, J. D. Hinnefeld, M. Huyse, C. Jouanne, V. Lapoux, A. Lépine, A. Lumbroso, F. Marie, A. Musumarra, G. Neyens, S. Ottini, R. Raabe, S. Ternier, P. Van Duppen, K. Vyvey, C. Volant, and R. Wolski, Phys. Rev. Lett. **84**, 2342 (2000).
[5] A. Di Pietro, P. Figuera, F. Amorini, C. Angulo, G. Cardella, S. Cherubini, T. Davinson, D. Leanza, J. Lu, H. Mahmud, M. Milin, A. Musumarra, A. Ninane, M. Papa, M. G. Pellegriti, R. Raabe, F. Rizzo, C. Ruiz, A. C. Shotter, N. Soic, S. Tudisco, and L. Weissman, Phys. Rev. C **69**, 044613 (2004).
[6] R. Raabe, J. L. Sida, J. L. Charvet, N. Alamanos, C. Angulo, J. M. Casandjian, S. Courtin, A. Drouart, D. J. C. Durand, P. Figuera, A. Gillibert, S. Heinrich, C. Jouanne, V. Lapoux, A. Lepine-Szily, A. Musumarra, L. Nalpas, D. Pierroutsakou, M. Romoli, K. Rusek, and M. Trotta, Nature **431**, 823 (2004).
[7] Yu. E. Penionzhkevich, V. I. Zagrebaev, S. M. Lukyanov, and R. Kalpakchieva, Phys. Rev. Lett. **96**, 162701 (2006).
[8] V. V. Flambaum and V. G. Zelevinsky, J. Phys. G **31**, 355 (2005).
[9] P. H. Stelson, H. J. Kim, M. Beckerman, D. Shapira, and R. L. Robinson, Phys. Rev. C **41**, 1584 (1990).
[10] J. F. Liang, D. Shapira, C. J. Gross, J. R. Beene, J. D. Bierman, A. Galindo-Uribarri, J. Gomez del Campo, P. A. Hausladen, Y. Larochelle, W. Loveland, P. E. Mueller, D. Peterson, D. C. Radford, D. W. Stracener, and R. L. Varner, Phys. Rev. Lett. **96**, 029903(E) (2006).
[11] W. Loveland, D. Peterson, A. M. Vinodkumar, P. H. Sprunger, D. Shapira, J. F. Liang, G. A. Souliotis, D. J. Morrissey, and P. Lofy, Phys. Rev. C **74**, 044607 (2006).
[12] M. Trotta, A. M. Stefanini, L. Corradi, A. Gadea, F. Scarlassara, S. Beghini, and G. Montagnoli, Phys. Rev. C **65**, 011601(R) (2001).
[13] A. M. Stefanini, F. Scarlassara, S. Beghini, G. Montagnoli, R. Silvestri, M. Trotta, B. R. Behera, L. Corradi, E. Fioretto, A. Gadea, Y. W. Wu, S. Szilner, H. Q. Zhang, Z. H. Liu, M. Ruan, F. Yang, and N. Rowley, Phys. Rev. C **73**, 034606 (2006).
[14] A. M. Borges, C. P. da Silva, D. Pereira, L. C. Chamon, E. S. Rossi Jr., and C. E. Aguiar, Phys. Rev. C **46**, 2360 (1992).
[15] H. Timmers, D. Ackermann, S. Beghini, L. Corradi, J. H. He, G. Montagnoli, F. Scarlassara, A. M. Stefanini, and N. Rowley, Nucl. Phys. **A633**, 421 (1998).
[16] M. S. Hussein, M. P. Pato, L. F. Canto, and R. Donangelo, Phys. Rev. C **46**, 377 (1992).
[17] L. F. Canto, R. Donangelo, P. Lotti, and M. S. Hussein, Phys. Rev. C **52**, R2848 (1995).
[18] T. Nakatsukasa, M. Ito, K. Yabana, and M. Ueda, AIP Conf. Proc. **853**, 291 (2006); M. Ito, K. Yabana, T. Nakatsukasa, and M. Ueda, Phys. Lett. **B637**, 53 (2006).
[19] A. Diaz-Torres and I. J. Thompson, Phys. Rev. C **65**, 024606 (2002).
[20] N. Takigawa and H. Sagawa, Phys. Lett. **B265**, 23 (1991).
[21] C. H. Dasso and A. Vitturi, Phys. Rev. C **50**, R12 (1994).
[22] K. Hagino, A. Vitturi, C. H. Dasso, and S. M. Lenzi, Phys. Rev. C **61**, 037602 (2000).
[23] C. Beck, A. Sanchez, I. Zafra, A. Diaz-Torres, I. J. Thompson, N. Keeley, and F. A. Souza, AIP Conf. Proc. **853**, 384 (2006).
[24] J. F. Liang and C. Signorini, Int. J. Mod. Phys. E **14**, 1121 (2005).
[25] L. F. Canto, P. R. S. Gomes, R. Donangelo, and M. S. Hussein, Phys. Rep. **424**, 1 (2006).
[26] V. Yu. Denisov, Eur. Phys. J. A **7**, 87 (2000).
[27] V. I. Zagrebaev, Phys. Rev. C **67**, 061601(R) (2003).
[28] G. Pollarolo and A. Winther, Phys. Rev. C **62**, 054611 (2000).
[29] D. L. Hill and J. A. Wheeler, Phys. Rev. **89**, 1102 (1953).
[30] K. Hagino, N. Rowley, and A. T. Kruppa, Comput. Phys. Commun. **123**, 143 (1999).
[31] V. I. Zagrebaev and V. V. Samarin, Phys. At. Nucl. **67**, 1462 (2004); CC fusion code of the NRV, http://nrv.jinr.ru/nrv/
[32] V. I. Zagrebaev, Y. Aritomo, M. G. Itkis, Yu.Ts. Oganessian, and M. Ohta, Phys. Rev. C **65**, 014607 (2002).
[33] W. von Oertzen, H. G. Bohlen, B. Gebauer, R. Künkel, F. Pühlhofer, and D. Schüll, Z. Phys. A **326**, 463 (1987).
[34] A. M. Stefanini, AIP Conf. Proc. **853**, 5 (2006).
[35] J. Blocki, J. Randrup, W. J. Swiatecki, and C. F. Tsang, Ann. Phys. (NY) **105**, 427 (1977).
[36] V. I. Zagrebaev, Prog. Theor. Phys. Suppl. **154**, 122 (2004).
[37] E. F. Aguilera, J. J. Kolata, F. M. Nunes, F. D. Becchetti, P. A. De Young, M. Goupell, V. Guimarães, B. Hughey, M. Y. Lee, D. Lizcano, E. Martinez-Quiroz, A. Nowlin, T. W. O'Donnell, G. F. Peaslee, D. Peterson, P. Santi, and R. White-Stevens, Phys. Rev. Lett. **84**, 5058 (2000).
[38] A. R. Barnett and J. S. Lilley, Phys. Rev. C **9**, 2010 (1974).
[39] W. Loveland, A. M. Vinodkumar, R. S. Naik, P. H. Sprunger, B. Matteson, J. Neeway, M. Trinczek, M. Dombsky, P. Machule, D. Ottewell, D. Cross, K. Gagnon, and W. J. Mills, Phys. Rev. C **74**, 064609 (2006).
[40] L. D. Landau and E. M. Lifshitz, *Mechanics* (Pergamon, New York, 1976), Vol. 1.
[41] V. I. Zagrebaev and V. V. Samarin, Yad. Fiz. **70**, No.6, 1 (2007).
[42] M. E. Riley and B. Ritchie, Phys. Rev. A **59**, 3544 (1999).
[43] T. Kajino, G. J. Mathews, and G. M. Fuller, Astrophys. J. **364**, 7 (1990).
[44] R. A. Malaney and W. A. Fowler, Astrophys. J. **333**, 14 (1988).